Formation of Pickering and mixed emulsifier systems stabilised O/W emulsions via confined impinging jets processing

Tripodi, Ernesto; Norton, I. T.; Spyropoulos, F.

DOI:
10.1016/j.fbp.2019.11.021

Document Version
Peer reviewed version

Citation for published version (Harvard):
Tripodi, E, Norton, IT & Spyropoulos, F 2020, 'Formation of Pickering and mixed emulsifier systems stabilised O/W emulsions via confined impinging jets processing', *Food and Bioproducts Processing*, vol. 119, pp. 360-370. https://doi.org/10.1016/j.fbp.2019.11.021

Formation of Pickering and mixed emulsifier systems stabilised O/W emulsions via Confined Impinging Jets processing

Ernesto Tripodi, I.T. Norton, F. Spyropoulos

School of Chemical Engineering, University of Birmingham, Edgbaston B15 2TT, Birmingham, UK

Highlights

- Confined impinging Jets have shown the potential to assist the processing of dilute and more concentrated emulsions at high levels of energy dissipation rate and low-energy inputs.
- The preparation of O/W emulsions stabilised by different concentrations of either Pickering particles alone or mixed emulsifier (surfactant and particles) formulations, using Confined Impinging Jets (CIJs), was investigated.
- The smallest droplet size was observed as progressively larger energy dissipation rates were approached, or upon multipassing through the CIIs geometry after the second passage.
- The combination of the emulsifiers aided in prolonging the emulsion stability upon storage, even at concentrations where each of them on their own do not give a stable emulsion microstructure.

Abstract

This study investigates for the first time the production of 10 and 40 wt.% oil-in-water emulsions stabilised by an array of particles and mixed emulsifier (Tween20-silica) concentrations. CIJs performance was evaluated for a range of hydrodynamic conditions (energy dissipation rates, $\bar{\varepsilon}_{th}$) and multipassing through the CIJs geometry followed by a monitoring of the emulsion storage stability. Overall, it was demonstrated that droplet size reduction was promoted as higher energy levels of $\bar{\varepsilon}_{th}$ were approached, regardless of the formulation. Following emulsion recirculation under fixed jet mass flow rate, the residence time associated with two passes was sufficient to ensure no further changes in terms of both average droplet size ($d_{3,2}$) and span of the droplet size distribution. Only when Tween20 and silica were mixed at low concentrations (0.01 and 0.10 wt.%, respectively), this emulsifier system could not promote any droplet size reduction upon both processing and multipassing. All systems showed excellent stability over 40 days of storage and it was possible to demonstrate that the combination of the emulsifiers aided in prolonging the emulsion stability. In conclusion, this investigation aims to extend the current range of emulsion microstructures that can be produced by CIJs to further enhance its industrial applicability.

Keywords: Pickering Emulsion; Mixed emulsifier system; Confined Impinging Jets.

1. Introduction

The emulsification performance of high-energy processing techniques (e.g. high-shear mixing, ultrasound treatment and high-pressure homogenisation) in the turbulent regime has been extensively investigated and characterised for a wide range of emulsion formulations (Rayner, 2015). In the turbulent regime (provided that there is enough emulsifier to stabilise the formed interfacial area), the final emulsion droplet size and droplet size distribution largely depend on the characteristic time scale of the emulsifier adsorption at the droplet interface (McClements and Jafari, 2018). Therefore, the selection of the emulsifier represents a crucial choice to ensure an efficient emulsification process (Donsì, 2018). Surfactants and nanoparticles (amongst others) represent common examples of emulsifier systems used to aid droplet stabilisation upon processing. Surfactants can usually adsorb at the droplet interface more rapidly than particles (Dickinson, 2012). What is more, once adsorbed at the interface, surfactants lower the interfacial tension, thus favouring droplet break-up (Kralova and Sjöblom, 2009). Conversely, although particles are not surface-active, Pickering emulsions have shown better resistance against droplet coalescence, which is realised by the particles' (almost) irreversible adsorption at the interface (Binks *et al.*, 2007;Chevalier and Bolzinger, 2013). The slower mechanism of particle adsorption at the interface additionally implies that droplet stabilisation is mainly driven by the capacity of the processing technique to achieve high levels of turbulence (Pichot *et al.*, 2009). These differences also explains why (during processing, under similar levels of turbulence) the emulsion droplet size of systems stabilised by surfactants is usually smaller (Tcholakova *et al.*, 2008). A possible strategy that could be employed to mitigate the differences in the droplet size between particle- and surfactant-stabilised emulsions is represented by adding a small amount of surface-active species during the processing of Pickering emulsions. It has been shown that by using such mixed emulsifier systems, it may be possible to combine the benefits deriving from the use of both species to produce emulsions with a smaller droplet size (than that of particle-stabilised systems) and with greater storage stability (than that of surfactant-stabilised systems) (Nesterenko *et al.*, 2014;Zafeiri *et al.*, 2017;Huang *et al.*, 2019).

Notwithstanding the consent of high-energy manufacturing methods for the high-throughput processing of small droplets, their major limitations are associated with the unavoidable waste of a large part of their energy input as dissipated heat, which makes these techniques energetically inefficient (Jafari *et al.*, 2008;Lee and Norton, 2013). Low-energy approaches, such as membrane or microfluidic emulsification, exploiting the spontaneous formation of droplets as a consequence of detachment from the membrane pore or a microchannel junction, overcome such energy efficiency problems since these do not rely on turbulence (Kobayashi *et al.*, 2004;Vladisavljević *et al.*, 2012). However, due to the very absence of turbulence, these techniques are less effective in promoting the transport of slower emulsifiers (such as particles) at the drop interface, often resulting in larger droplet sizes. Furthermore,

their development for larger-scale production still faces the major challenge of achieving high throughputs (Kobayashi *et al.*, 2004;Vladisavljević *et al.*, 2012).

In contraposition, Confined Impinging Jets (CIJs) have shown the potential of overcoming both of these limitations. In CIJs two (either the pure oil and water phases or two pre-emulsion) jets collide at high velocities within a confined geometry (Tripodi *et al.*, 2019). CIJs exploit the energy dissipated upon impingement as the driving force for the turbulent production of emulsions rather than the application of high-levels of shearing, pressure or cavitation (Tripodi *et al.*, 2019). Due to the confined mixing volume, droplets experience rather uniform disruptive forces, resulting in the high throughput production of emulsions with tailored microstructural features (e.g. droplet size and droplet size distribution) (Chiou *et al.*, 2008). The energy dissipation rate generated upon jet collision can be theoretically estimated (Siddiqui *et al.*, 2009) according to:

$$\bar{\varepsilon}_{th} = \frac{2\, Q_{jet}\, \Delta P}{\rho V_{CIJs}} \quad (1)$$

where Q_{jet} is the jet flow rate, ΔP is the pressure at which jet collision takes place, ρ is the density of either the pure phase in each jet or the pre-emulsion, and V_{CIJs} is the volume within the CIJs geometry where jet collision and mixing occur.

Emulsification using CIJs represents a relatively new area of research and as a consequence the literature on this topic is still somewhat limited. CIJs processing of dilute emulsions (volume fractions < 10 vol.%) has been evaluated for a range of different emulsifiers (Tween20, Span80, Whey Protein, Lecithin or Sodium Dodecyl Sulphate), hydrodynamic conditions (jet flow rates) and residence times (including recirculation through the mixing chamber) (Siddiqui and Norton, 2012). It was observed that the smallest droplet size (~2 μm) was achieved approaching the highest jet flow rates, independently from the type of surfactant used. More recently, it has also been shown that CIJs processing allowed the production of dilute emulsions having an average droplet dimension within the nano-size range (~700 nm) but only if coupled with an ultrasound treatment (Siddiqui *et al.*, 2017). An additional study investigated the use of CIJs for the production of emulsions with dispersed phase content up to 80%, in the surfactant (Tween20)-poor and -rich regime, hydrodynamic conditions as well as residence times (Tripodi *et al.*, 2019). In this work, CIJs operation could induce droplet size reduction only when the process took place within the identified optimal processing window (i.e. mass jet flow rate, W_{jet} , > 176 g/min) and pre-emulsions were prepared with an average droplet size above a certain threshold (~10 μm). The CIJs emulsification performance remained almost unaffected upon variation of the dispersed phase mass fraction with all emulsions reaching their lowest droplet size (~ 8μm) when processed under the highest W_{jet}, regardless of the surfactant concentration. Furthermore, recirculation (up to 4 passes) within the CIJs cavity under fixed W_{jet} produced as an effect the narrowing of the emulsions droplet size distribution with minor variations in their average droplet size.

Despite the CIJs potential to assist in the formation of dilute as well as more concentrated emulsions with small droplet sizes at high levels of turbulence and at low-energy inputs, no studies (to the best of the authors' knowledge) have previously reported on the assessment of the CIJs emulsification performance in producing Pickering and mixed-emulsifier (surfactant and particles) stabilised O/W emulsions. Thus, this study reports for the first time on the use of CIJs to process dilute (10 wt.%) as well as semi-concentrated (40 wt.%) emulsions stabilised by either particles or mixed emulsifier systems. The emulsion microstructure was evaluated in terms of final droplet sizes and droplet size distributions resulting from both exposure to a range of CIJs hydrodynamic conditions and multi-passing (recirculation) through a fixed turbulent environment. Emulsion stability was also assessed following a storage period of 40 days.

Overall, the present study aims to extend the current spectrum of emulsion microstructures that can be produced by CIJs, thus building upon the process's lower-energy credentials and capacity to deliver high product throughputs to further enhance its industrial applicability.

2. Materials and Methods

2.1. Materials

All oil-in-water (O/W) emulsions were prepared by using de-ionised water obtained from a reverse osmosis filtration system as the continuous phase. Commercial sunflower oil (viscosity = 50 cP) was purchased by a local retailer and used as the dispersed phase. Both Polysorbate20, i.e. Tween20, (Hydrophilic Lipophilic Balance, HLB =16.70 and molecular weight=1227.54 g/mol, critical micelle concentration = 0.06 mM) and a 30 wt.% suspension of silica in Water (Ludox HS, surface area 220 m^2/g and density 1.21 g/mL) were supplied by Sigma-Aldrich Company (UK) and used as emulsifiers.

2.2. Methods

2.2.1. Dispersion and characterisation of silica particles in water

For the preparation of the silica-in-water dispersion, the 30wt.% Ludox solution was added to the continuous phase and their quantity adjusted accordingly to reach the desired particle concentration (0.10 to 5 wt.% of the total emulsion weight, i.e. 500 g). The initial pH of the solution (~10) was then lowered to ~2 using the required quantities of hydrochloric acid (HCl, 1M) and sodium hydroxide (NaOH, 1M). It has been shown that to produce effective stabilisation of O/W emulsions, it is possible to modify the surface character of hydrophilic silica by lowering the pH of the aqueous medium to 2 (Dickinson, 2010). The silica particle size, particle size distribution and ζ-potential were then characterised at 22°C by using a dynamic light scattering analysis technique, Zetasizer (Malvern

Instruments). Each experiment was repeated three times. Figure 1 shows the effect of the variation in pH on the above parameters. The particle size remained (practically) unaffected over the entire range of pH. Upon the reduction of the pH from 10 to 2, the particle size distribution became slightly narrower while the zeta potential strongly decreased from - 45 mV to 0 mV (e.g. isoelectric point), respectively.

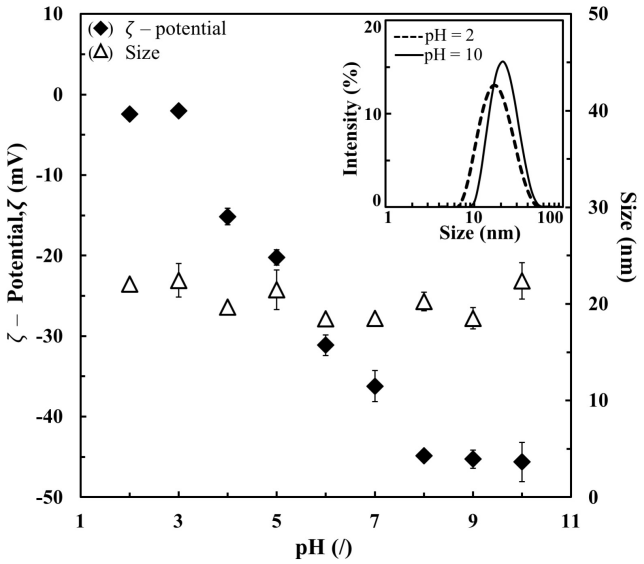

Figure 1. Silica particle size (△) and ζ-potential (◆) varying as a function of the pH. All data points are mean values (n=3) and error bars are reported as a single standard deviation. Where not visible error bars result smaller than symbols. (Inset Graph) Particle size distributions resulting from the reduction of the pH from 10 (solid line) to 2 (dashed line) of the silica-in-water dispersion.

2.2.2. Emulsion preparation

Emulsions were prepared following a two-step procedure, which included: *(i)* high-shear mixing to form the initial coarse pre-emulsion followed by *(ii)* emulsification within the Confined Impinging Jets (CIJs) device.

2.2.2.1. Pre-emulsion preparation

2.2.2.1.a. Preparation of nano-particle stabilised O/W pre-emulsions

The required amount of vegetable oil (10% or 40 % of the total emulsion weight, i.e. 500 g) was added to the silica-in-water dispersion (prepared as described in Section 2.2.1). Sunflower oil and the silica-in-water solution were then pre-emulsified by means of a Silverson L5 Series Laboratory High-Shear Mixer, equipped with an emulsor screen of 33 mm in diameter, for 3 min at 2000 RPM. It should be noted that the pre-emulsification conditions were chosen in order to obtain a stable to-be-processed pre-emulsion but with a droplet size large enough to be manufactured via the Confined Impinging Jets. In a forthcoming study, comparing the processing performance of various emulsification techniques, we

found that the overall CIJs energy input resulted practically unaffected by the presence of the pre-emulsification stage

2.2.2.1.b. Preparation of mixed emulsifier stabilised O/W pre-emulsions

The required concentration of Tween20 (0.01 or 0.1 wt.% of the total emulsion weight, i.e. 500 g) was dissolved in the silica-in-water dispersion (prepared as described in Section 2.2.1) by using a magnetic stirrer for 10 min, before the addition of the desired amount of sunflower oil (10% or 40% of the total emulsion weight). The silica-in-water dispersion, Tween20 and the vegetable oil were then pre-emulsified by means of a Silverson L5 Series Laboratory High-Shear Mixer, equipped with an emulsor screen of 33 mm in diameter, for 3 min at 2000 RPM.

2.2.2.2. CIJs processing

As the second stage, the pre-emulsions were processed through the CIJs geometry, Figure 2 , by means of a single pulse-less micro-pump (external gear pump) with jet mass flow rates varying from 85.50 to 702 g/min. Prior impingement the flow was split into two equal streams by using a Y-junction, whereas after leaving the CIJs chamber, emulsions samples were collected and stored in sample pots.

To study the effect of multipassing, emulsions were processed through the CIJs under fixed inlet mass jet flow rate (352.75 g/min) and were collected in a beaker. This was then transferred back to the feed and the formed emulsion was re-processed up to 4 times. Each experiment was repeated twice.

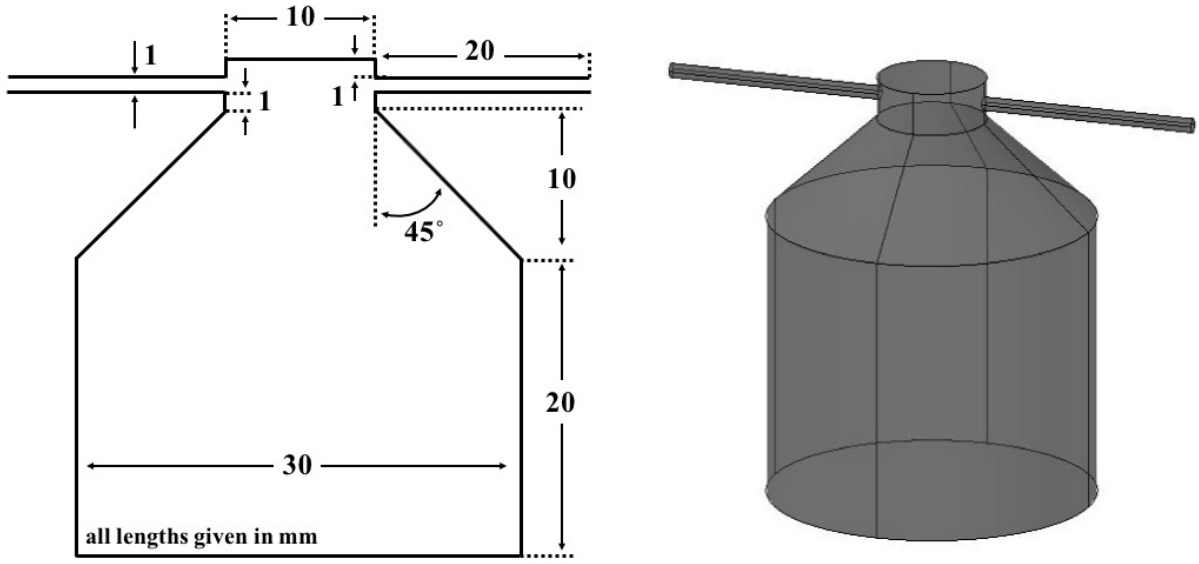

Figure 2. Schematic and three-dimensional representation of the CIJs geometry employed in this study; all dimensions are given in millimetres.

2.2.3. Droplet size measurements

The measurement of droplet size and droplet size distribution were carried out by using a Mastersizer 2000 (Malvern Instruments). Samples were diluted to 3 vol.% in order to avoid multiple-light scattering. Within the Mastersizer, samples were tested three times at room temperature (22˚C) and an average was calculated. Each experiment was repeated twice.

2.2.4. Interfacial tension measurements

The equilibrium interfacial tensions (γ) of the O/W interface both without and with emulsifier systems at varying concentration were measured using a K11-Force Tensiometer (Krüss, GmbH) equipped with a Wilhelmy plate at room temperature (22°C). Table 1 shows that the interfacial tension of the plain sunflower oil-water interface resulted equal to 24.95 ± 0.02 mN/m in excellent agreement with the literature values. Upon variation of the silica concentration from 0.10 to 5 %, the O/W interfacial tension slightly deviated from the plain O/W γ, decreasing from 24.51 ± 0.03 to 20.41 ± 0.01, respectively. This minimal reduction may be addressed to the presence of surface-active contaminants associated with the particle solution (Binks *et al.*, 2007). With the addition of (0.01 and 0.1 wt.%) Tween20 to (0.10 and 1wt.%) silica, the γ dropped to similar values shown for the interfacial tensions of the O/W interface solely stabilised by Tween20, according with the results observed in the literature.

Table 1. Equilibrium interfacial tension, γ, of the emulsifier systems used in this study. [a]Equilibrium interfacial tension of the oil/water system deprived on any emulsifier.

Silica (wt.%)	Tween20 (wt.%)	γ (mN/m)
0[a]	0[a]	24.95 ± 0.02 [a]
0.10	0	24.51 ± 0.03
1	0	24.30 ± 0.02
2	0	22.60 ± 0.02
5	0	20.41 ± 0.01
0	0.01	6.04 ± 0.01
0	0.10	5.34 ± 0.02
0.10	0.01	6.60 ± 0.03
1		4.82 ± 0.03
0.10	0.10	4.58 ± 0.02
1		4.13 ± 0.03

2.2.5. Stability

Samples were stored in the laboratory at room temperature (22°C) over a period of 40 days to evaluate the long-term emulsion stability. Since creaming occurred in most of the sample analysed in this study, the samples were gently re-dispersed before re-measuring their droplet size and droplet size distribution.

3. Results and discussion

3.1. O/W emulsions solely stabilised by particles

The effect of varying the silica concentration on the average droplet size ($d_{3,2}$) of both 10 wt.% and 40 wt.% O/W pre-emulsions processed through the CIJs under varying hydrodynamic conditions is presented in Figure 3. CIJs hydrodynamic conditions are expressed in terms of the theoretically estimated energy dissipation rate, $\bar{\varepsilon}_{th}$, according to eq. 1. Silica concentrations of 0.10, 1, 2 and 5 wt.% were used for the preparation of all pre-emulsions, although systems with a high dispersed phase content (40 wt.%) and low particle concentration (0.10 wt.%) rapidly phase separated following pre-mixing and thus processing through the CIJs was not performed.

The data presented in Figure 3.A for the 10 wt.% oil pre-emulsions shows that the droplet sizes for these systems were practically the same for silica concentrations up to 2 wt.%, whereas a small size reduction occurred for pre-emulsions containing 5 wt.% silica. Since the pre-mixing stage conditions during the production of all systems were the same, the pre-emulsion droplet size decrease is most likely associated with an increased particle interfacial adsorption rate facilitated by the higher silica concentration. However, once the dispersed phase fraction was increased to 40 wt.% and thus the interfacial area became larger, the pre-emulsion droplet size was independent of silica concentration (Figure 3.B).

The pre-emulsions were then processed through the CIJs device using a range of hydrodynamic conditions. The $d_{3,2}$ variation with the $\bar{\varepsilon}_{th}$ demonstrated a common trend among the different formulations and oil mass fractions (Figure 3). At low values of $\bar{\varepsilon}_{th}$ ($< 2\times10^3$ W/kg), the pre-emulsion average droplet size was practically unaffected by the flow conditions within the CIJs chamber. Under these low $\bar{\varepsilon}_{th}$ conditions, all the systems maintained a similar identity to their respective pre-emulsions with variations in droplet size (Figure 3.A) contained within the experimental error. On the other hand, as the $\bar{\varepsilon}_{th}$ increased (highlighted areas in Figure 3), the droplet size reduction became more pronounced and all systems reached the lowest droplet size (~10 μm) at the highest value of $\bar{\varepsilon}_{th}$ regardless of particle concentration and oil content. In a recently published study (Tripodi *et al.*, 2019), it was demonstrated that the jet collision was compromised at low $\bar{\varepsilon}_{th}$, resulting in relatively poor mixing conditions and ultimately impeding CIJs emulsification capacity (within this energy dissipation rate range) . Contrarily, as higher levels of $\bar{\varepsilon}_{th}$ are approached (i.e. optimal processing conditions), the droplet size of (surfactant-stabilised) emulsions steeply decreased reaching its minimum value (~10μm) at the highest $\bar{\varepsilon}_{th}$. Although, the silica nanoparticles used in this study had an average diameter equal to ~20 nm (Figure 1), there are numerous reports suggesting that the particulate entities actually involved in the mechanism of droplet stabilisation are silica aggregates of mean diameter 100 nm and above (Hunter *et al.*, 2008; Leal-Calderon and Schmitt, 2008). What is more, particles (or their aggregates) can only effectively stabilise and prevent the recoalescence of emulsion droplets having a size at least ten times larger

(Binks, 2002; Tcholakova *et al.*, 2008; Dickinson, 2010). It is therefore reasonable to expect that upon processing stable emulsion droplet sizes with an average diameter above 1 μm are to be expected (Figure 3).

The span values of all CIJs produced emulsions exhibited the same response with respect to $\bar{\varepsilon}_{th}$, a behaviour which was in fact independent of particle concentration (inset graphs in Figure 3). Within the region of deficient operation, the span values remained rather similar to those of the corresponding pre-emulsions, further suggesting that pre-emulsion microstructure remains practically unchanged when processing at such low jet flow rates. However, in the optimal CIJs processing window (highlighted area), all span values exhibit a similar increase; droplet size distributions became progressively broader at higher energy dissipation rates. This is in agreement with the findings observed in the literature focusing on the performance of other emulsification techniques, which also explains why as a common practice recirculation is often required to reach the desired emulsion microstructure (Walstra, 1993;McClements, 2016).

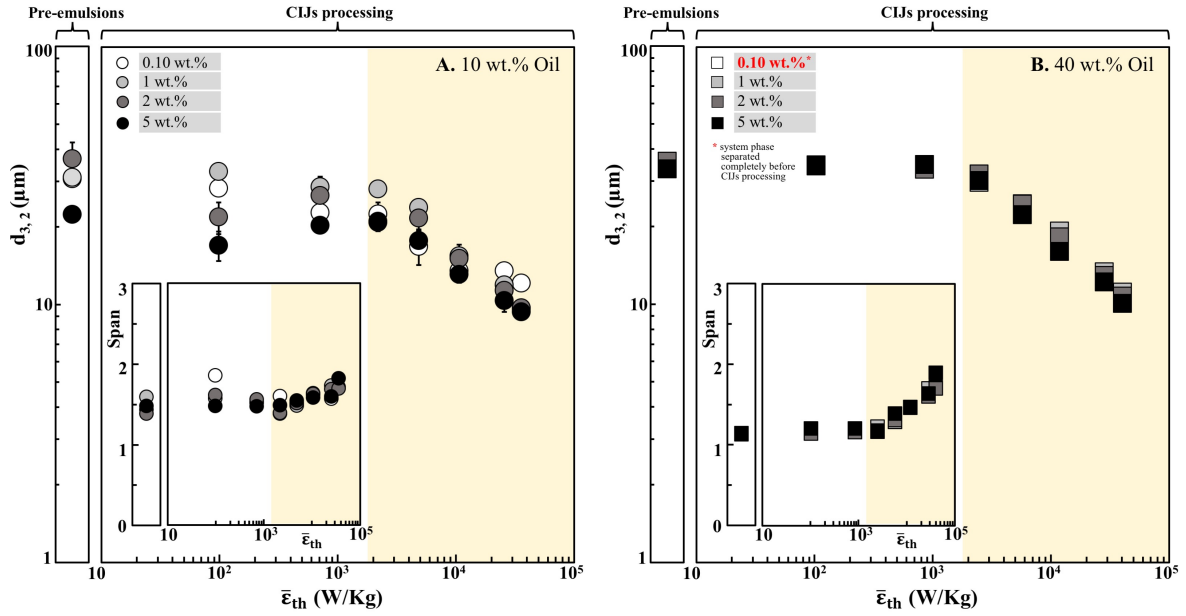

Figure 3. Emulsion Sauter diameter ($d_{3,2}$) as a function of the theoretically predicted energy dissipation rate ($\bar{\varepsilon}_{th}$; eq. 1) following CIJs processing of pre-emulsions with 10 wt.% (A) and 40 wt.% (B) oil mass fractions in the presence of an array of silica particles, ranging in concentration from 0.10 to 5 wt.%. Also shown (inset graphs), span values as a function of $\bar{\varepsilon}_{th}$. Highlighted areas in both the main and the inset graphs represent optimal CIJs processing conditions. All data points are average values (n=6) and error bars represent one standard deviation. Where not visible error bars are smaller than symbols.

3.2. O/W emulsions stabilised by mixed-emulsifier systems

Figure 4 shows the effect of $\bar{\varepsilon}_{th}$ on the Sauter diameter ($d_{3,2}$) of 10 wt.% and 40 wt.% O/W emulsions stabilised by surfactant–particle (Tween20-silica) mixed-emulsifier systems. Tween20

concentrations of 0.01 or 0.10 wt.% were combined with either 0.10 or 1 wt.% silica to form 10 wt.% (Figure 4.A and C) and 40 wt.% (Figure 4.B and D) O/W pre-emulsions which were subsequently processed through the CIJs. Figure 4 also includes $d_{3,2}$ versus $\bar{\varepsilon}_{th}$ data for emulsions stabilised solely by the equivalent concentrations (to those in the mixed-emulsifier system) of either the surfactant or particle species alone.

The variation of the $d_{3,2}$ of the 10 wt.% O/W emulsions stabilised by 0.01 wt.% of Tween20 and 0.10 or 1 wt.% of silica with the $\bar{\varepsilon}_{th}$ is presented in Figure 4.A. As observed in the previous section, both 0.10 and 1 wt.% particle-stabilised emulsion $d_{3,2}$ retained their pre-emulsion identity at low $\bar{\varepsilon}_{th}$ before being reduced to a minimum value of ~10 μm within the optimal processing window. Differently, the $d_{3,2}$ of the emulsion solely stabilised by the surfactant (0.01 wt.% of Tween20) was initially subjected to an increase, probably due to a combination of both the CIJs poor mixing efficiency at low $\bar{\varepsilon}_{th}$ and the fact that surfactants provide a less robust interface than particles (Binks, 2002;Aveyard *et al.*, 2003). Nonetheless, under efficient CIJs operation, the $d_{3,2}$ then followed similar trend and values than those showed by Pickering systems. Once surfactant and particles were mixed together at low concentrations (0.01 and 0.10 wt.% respectively), the $d_{3,2}$ exhibited a different dependency with the $\bar{\varepsilon}_{th}$. The Sauter diameter fluctuated around an average value of ~ 40 μm and no deviation from this trend was observed across the entire range of $\bar{\varepsilon}_{th}$. The addition of a surfactant to particle-system (or vice versa) can either enhance or undermine their efficiency as emulsifiers depending on both their type and relative concentration (Pichot *et al.*, 2009;Nesterenko *et al.*, 2014;Zafeiri *et al.*, 2017). It appears that, once mixed at low concentrations, the particles-surfactant system could not induce an effective stabilisation during CIJs processing regardless of the hydrodynamic conditions. Contrarily, as the particle concentration was increased to 1 wt.%, the Sauter diameter showed an initial increase to then undergo a steep reduction as the CIJs was operated under full capacity, in alignment with the trend observed with the systems stabilised by the single emulsifiers. The results suggest that the increase in the particle concentration induced a more efficient droplet stabilisation during processing thus resulting in the observed trend similar to that of the emulsions stabilised by the sole particles or surfactant.

Analogous trends were observed as the dispersed phase content was increased to 40 wt.%, Figure 4.B. The diameter of emulsions stabilised by the sole particles or surfactant decreased at increasing $\bar{\varepsilon}_{th}$ to reach a minimum value (~12 and 18 μm, respectively) as a higher $\bar{\varepsilon}_{th}$ was approached. For the mixed emulsifier systems, the $d_{3,2}$ of the low silica concentration co-stabilised emulsion remained constant at low values of $\bar{\varepsilon}_{th}$. Within the optimal operation region, the Sauter diameter was initially reduced followed by a rapid increase as the processing conditions became progressively more severe. Overall, despite higher energy dissipation conditions create favourable conditions for droplet size reduction, as this tendency increases (i.e. at further higher $\bar{\varepsilon}_{th}$), the observed raise in the $d_{3,2}$ suggests that the mixed emulsifier system could not efficiently stabilise emulsion droplets (strongly in agreement with the results of Figure 4.A), thus very likely resulting in their coalescence (i.e. in the shown $d_{3,2}$ increase).

Differently, at a higher particle concentration, the emulsion Sauter diameter remained fairly constant within the low energy dissipation rate region to then decrease to a minimum value (~20 μm) within the optimal CIJs operating window, following the trend of the emulsions stabilised by the single emulsifiers and similarly to the trend observed in Figure 4.A. Overall (with exception of the low particle co-stabilised emulsions), the processing conditions established during CIJs operation were such to minimise the differences in formulation (i.e. type and concentration of emulsifier as well as of the interfacial tension, Table 1) among the different systems investigated for both dispersed phase mass fractions.

Any possible variation in the Sauter diameter arising from the use of different emulsifier(s) was minimised once the Tween20 concentration was increased to 0.10 wt.% for both dispersed phase mass fractions, Figure 4.C and D. For the 10 wt.% O/W emulsions (Figure 4.C) stabilised by mixed emulsifiers, the $d_{3,2}$ did not significantly vary across the different formulations (either stabilised by mixed or sole emulsifier systems). In agreement with the trend observed in Figure 3 and Figure 4.A-B, the $d_{3,2}$ remained fairly constant before being reduced within the optimal operating window. All the systems showed a similar droplet size reduction as well as a similar smallest droplet size (~ 10 μm) achieved at the highest level of $\bar{\varepsilon}_{th}$.

Once the dispersed phase content was increased to 40 wt.% (Figure 4.D), emulsions practically retained their (original pre-emulsion) droplet diameter at low $\bar{\varepsilon}_{th}$, before undergoing a sharp reduction within the optimal processing window, and reaching a fairly similar $d_{3,2}$ (~10-15 μm) at the highest $\bar{\varepsilon}_{th}$ value, independently on the formulation.

With exception of the low-particle stabilised systems for both oil load contents, overall it appears that the CIJs hydrodynamic conditions, i.e. the energy dissipation rate, are the main parameter affecting the final emulsion droplet size.

The microstructural properties of emulsions stabilised by mixed surfactant-particles systems display an array of behaviour depending on their synergistic interactions, that in turn are affected by the type and relative concentration of emulsifiers as well as on the selected processing method (Ravera *et al.*, 2008). An earlier study demonstrated that the combination of silica and Tween20, at concentrations (3 and 0.10 wt.%, respectively) where each of them gave unstable (50 wt.%) castor O/W emulsions, resulted in stable systems after processing (Midmore, 1998). A previous investigation reported the displacement of nano-particles from the oil-water interface by surfactant molecules with the application of shear, when the surfactant was used at concentration above its critical micellar concentration (Vashisth *et al.*, 2010). Conversely, in another study the authors showed that the coupling of a non-ionic surfactant (monoolein) with silica nanoparticles during high-shear mixing improved the long-term stability of O/W emulsion through a two-stage synergistic mechanism (Pichot *et al.*, 2009). Overall, it is clear that drawing general conclusions about the stabilisation mechanisms of mixed

emulsifier systems is extremely challenging and their behaviour largely depends (amongst other factors) on the specific formulation and processing parameters.

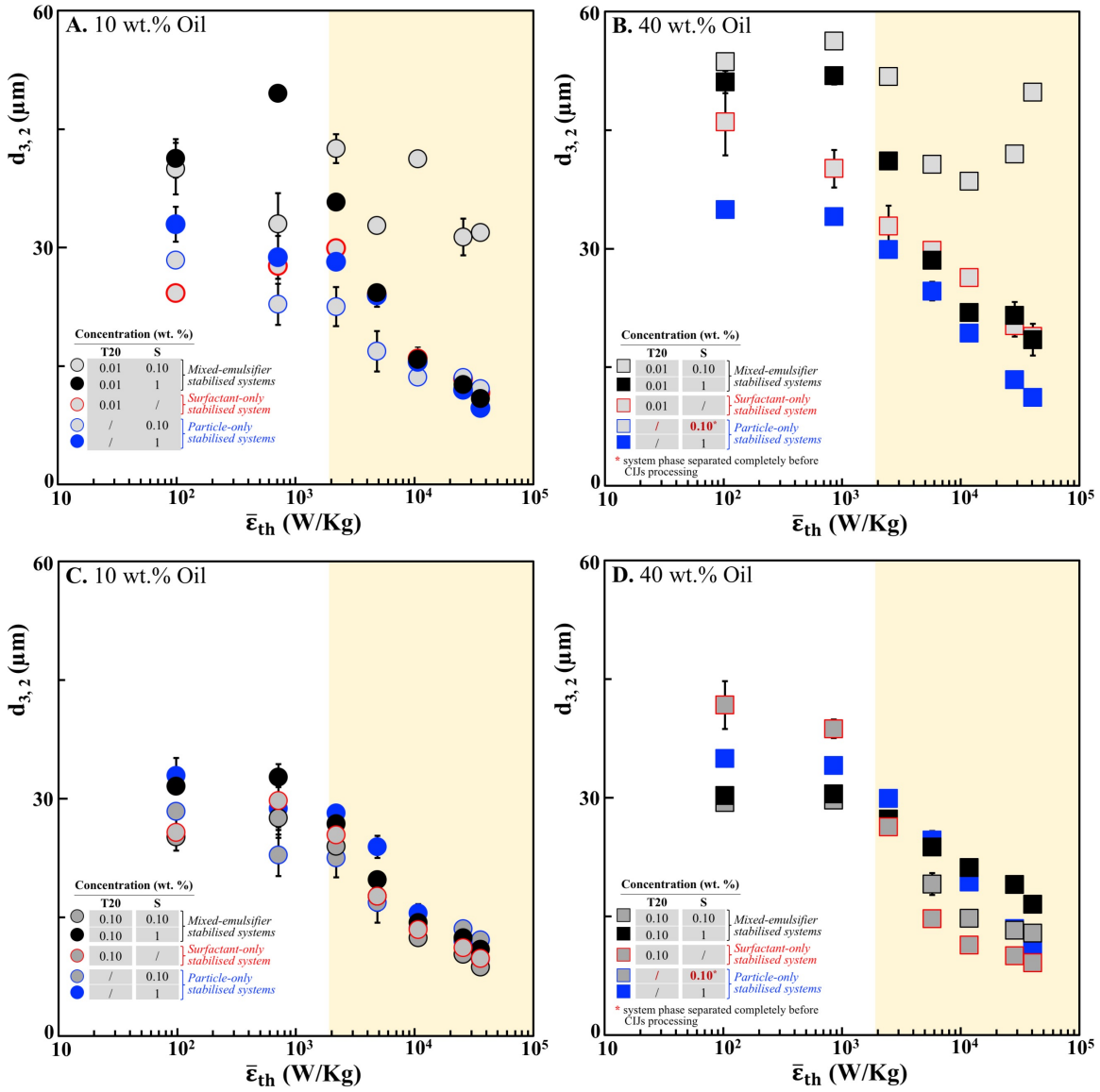

Figure 4. Emulsion Sauter diameter ($d_{3,2}$) as a function of the theoretically predicted energy dissipation rate ($\bar{\varepsilon}_{th}$; eq. 1) following the CIJs processing of pre-emulsions with 10 wt.% (A and C) and 40 wt.% (B and D) oil mass fractions, in the presence of mixed emulsifier (Tween20 and silica) systems; emulsifier concentrations are given in each figure legend. Also shown are the $d_{3,2}$ versus $\bar{\varepsilon}_{th}$ data for CIJs processed pre-emulsions stabilised solely by either of the two species in the mixed emulsifier systems alone. Highlighted areas represent the range of $\bar{\varepsilon}_{th}$ corresponding to optimal CIJs operation. All data points are mean values (n=6) and error bars are reported as a single standard deviation. Where not visible error bars result smaller than symbols.

3.3. Effect of CIJs recirculation

During operation of traditional emulsification techniques (e.g. high-pressure homogeniser, microfluidiser), emulsion droplets experience a wide range of disruptive forces upon a single pass, possibly resulting in larger average droplet sizes and/or broader droplet size distributions (Lee and

Norton, 2013). As a consequence, if both smaller droplets and narrower droplet size distributions are required, it is usually necessary to recirculate emulsions through the emulsification apparatus a number of times (Floury *et al.*, 2000;McClements, 2016).

The effect of the residence time on the emulsion Sauter diameter ($d_{3,2}$) and the span of the droplet size distribution was explored by the recirculation of all systems through the CIJs device for a total of 4 passes. Multi-passing was conducted under a single jet flow rate of 352.75 g/min corresponding to fixed hydrodynamic conditions with an $\bar{\varepsilon}_{th}$ value of $\sim 5\times10^3$ W/kg for both the 10 and 40 wt.% O/W emulsions. The selected jet flow rate is within the range of optimal CIJs operation but at the same time not significantly high as to overshadow any formulation-driven droplet size potential differences.

The change of the 10 wt.% O/W emulsion droplet size and span stabilised by 0.01 wt.% of Tween20 and 0.10 or 1 wt.% of silica as a function of the number of passes through the CIJs is presented in Figure 5.A. When both emulsifiers were used at low concentrations (0.01 wt.% Tween20 and 0.10 wt.% silica), the $d_{3,2}$ remained unaffected by the recirculation in the CIJs device. This result confirms, in line with the findings shown in Figure 4.A, that this couple of emulsifiers (used at these concentrations) could induce no droplet size reduction, even after spending a prolonged time within the high energy dissipation region of the CIJs.

However, as the silica concentration was increased to 1 wt.% (at fixed 0.01 wt.% of Tween20), the average droplet size reached its minimum value after the second pass with no other changes taking place upon further recirculation, similarly to the emulsions solely stabilised by the two emulsifiers alone. It is also worth mentioning that the span values of the droplet size distributions remained fairly constant as a function of the number of passes, with negligible differences between the different emulsifier systems.

The effect of the recirculation on both the $d_{3,2}$ and the span values of emulsions with a higher oil load (40 wt.%) were also evaluated (Figure 5.B). In this case the increase in interfacial area exacerbated the poor stabilisation efficiency of the mixed system with the lowest concentration of emulsifiers (0.01 wt.% Tween20 and 0.10 wt.% silica). In fact, the Sauter diameter increased as a result of recirculation from ~40μm (first pass) to ~60μm (third pass),and remained constant after then. These findings align with the trend observed in Figure 4.B. While in that case, the average droplet size increases as a consequence of exposing the emulsion to a progressively increasing $\bar{\varepsilon}_{th}$, equivalently during multi-passing, the $d_{3,2}$ increases as a result of exposing the emulsion for a longer time under fixed $\bar{\varepsilon}_{th}$. For mixed emulsifier systems with a higher particle concentration (1 wt.%), the resulting Sauter diameter did not change after the second pass, with $d_{3,2}$ values being rather close to the ones for emulsions solely stabilised by either of the emulsifiers alone. The span values of the distributions (similarly to the trend shown in Figure 5.A) remained practically constant over each pass and were largely similar across the different formulations.

As the Tween20 concentration in the mixed emulsifier system was increased to 0.10 wt.%, differences in the $d_{3,2}$ values for emulsions containing either 10 wt.% or 40 wt.% dispersed phase became negligible (Figure 5.C and D, respectively). The minimum droplet size was realised after the second pass while the span values remained constant with increasing residence time within the CIJs turbulent environment, regardless of whether emulsions were stabilised by mixed or sole emulsifier formulations.

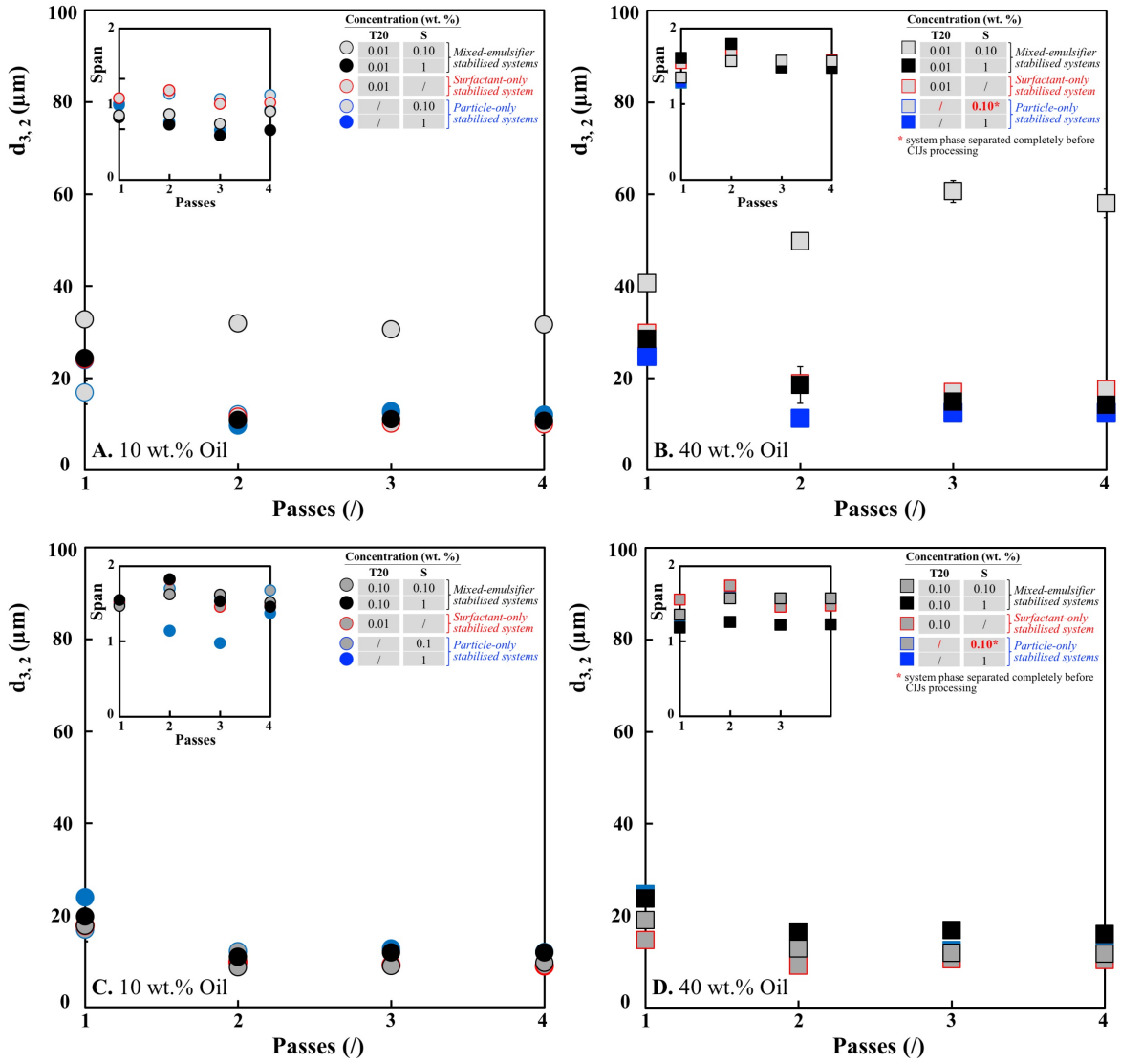

Figure 5. Emulsion Sauter Diameter ($d_{3,2}$) and span values (inset graphs) as a function of the number of passes through the CIJs geometry (at a fixed mass jet flow rate of 352.75 g/min corresponding to fixed hydrodynamic conditions with an $\bar{\varepsilon}_{th}$ (eq.1) value of ~5×10^3 W/kg) for both the 10 (A-C) and 40 (B-D) wt.% dispersed phase contents, in the presence of mixed emulsifiers; emulsifier concentrations are given in each figure legend. Also shown are the $d_{3,2}$ versus the number of passes data for CIJ processed pre-emulsions stabilised solely by either of the two species in the mixed emulsifier systems alone. All data points are mean values (n=6) and error bars are reported as a single standard deviation. Where not visible error bars result smaller than symbols.

Other studies on CIJs reported that the droplet size distributions of emulsions with much lower (to those investigated here) dispersed phase contents (up to a volume fraction of 0.10) was the major parameter affected by recirculation (Siddiqui and Norton, 2012). Similarly, other studies evaluating the emulsification capacity of a high-pressure homogeniser or microfluidiser concluded that the droplet size distribution was the major emulsion microstructural feature affected by the multi-passing (Karbstein and Schubert, 1995;Tesch *et al.*, 2002;Qian and McClements, 2011). Recirculation is often necessary in traditional emulsification practice because due to the large volumes where homogenisation takes place, droplets experience largely non-uniform disruptive forces, thus possibly resulting in a larger average droplet diameter and/or broader droplet size distribution. One of the possible advantages of using CIJs lies in its small volume, which allows to most of the droplets to pass through the high-energy dissipation region without bypassing it (Siddiqui *et al.*, 2009). In the present study, both emulsion droplet size and span remained practically unaffected after the second pass, thus suggesting that the residence time associated with two passes is sufficient to ensure that the generated hydrodynamic conditions are experienced by the entirety of the sample volume under processing. In addition, by looking at the different impact of either (an increasing) $\bar{\varepsilon}_{th}$ or recirculation (at fixed $\bar{\varepsilon}_{th}$) on the $d_{3,2}$ (Figure 3 and 4), this could also hint that the magnitude of the energy dissipation rate affect the microstructure of the different emulsions more than its duration.

3.4. Long-term emulsion stability

The stability of all emulsions produced after a single pass in the CIJs geometry (at a fixed $\bar{\varepsilon}_{th}$ value of ~5 $\times 10^3$ W/kg) was monitored at room temperature (22°C) over a storage period of 40 days. Figure 6 and Figure 7 present the emulsion average diameters ($d_{3,2}$) upon formation in the CIJs device and after 40 days of storage, for systems stabilised by silica alone (Figure 6) or by the mixed (Tween20 and silica) emulsifier formulations (Figure 7); in each case data for both the 10 wt.% and 40 wt.% dispersed phase contents are given.

The $d_{3,2}$ data of 10 wt.% oil content emulsions stabilised by silica particles alone (Figure 6.A) clearly demonstrated the high stability of these systems. Their Sauter diameter, regardless on the concentration of particles used, remained practically unaltered after the 40 days of storage. This is also confirmed by the negligible changes to the droplet size distribution over the same storage period (inset in Figure 6.A). Emulsion stability was also maintained for the 40 wt.% dispersed phase content systems (Figure 6.B) stabilised by silica at concentrations equal and greater to 1 wt.%. Pre-emulsions containing 0.10 wt.% silica rapidly underwent phase separation prior to CIJs processing and thus have not been included here.

A similar behaviour was also exhibited by the 10 wt.% oil content emulsions stabilised by the mixed emulsifier systems (Figure 7.A). Both the Sauter diameters and droplet size distributions for these systems remained unaltered during storage.

As the dispersed phase content was increased to 40 wt.%, emulsion stability was retained for all mixed emulsifier concentrations except for the lowest one; 0.01 wt.% Tween20 and 0.10 wt.% silica (Figure 7.B). For these systems, the $d_{3,2}$ increased from ~40 µm (after CIJs processing) to ~60 µm (at the end of the storage period). It should be highlighted that, as previously discussed, the pre-emulsions containing 0.10 wt.% silica phase separated immediately after their preparation, whereas, in our previous work, we showed that although the emulsions stabilised by only 0.01 wt.% Tween20 remained stable after CIJs processing ($d_{3,2}$ ~ 25µm), these phase separated during the storage period, i.e. 40 days (Tripodi *et al.*, 2019). Thus, there is a clear evidence that the combination of the emulsifiers (even at concentrations where each of them on their own do not give a stable emulsion microstructure) aids in prolonging the emulsion stability, although in this case the droplet size was not entirely retained (Figure 7.B).

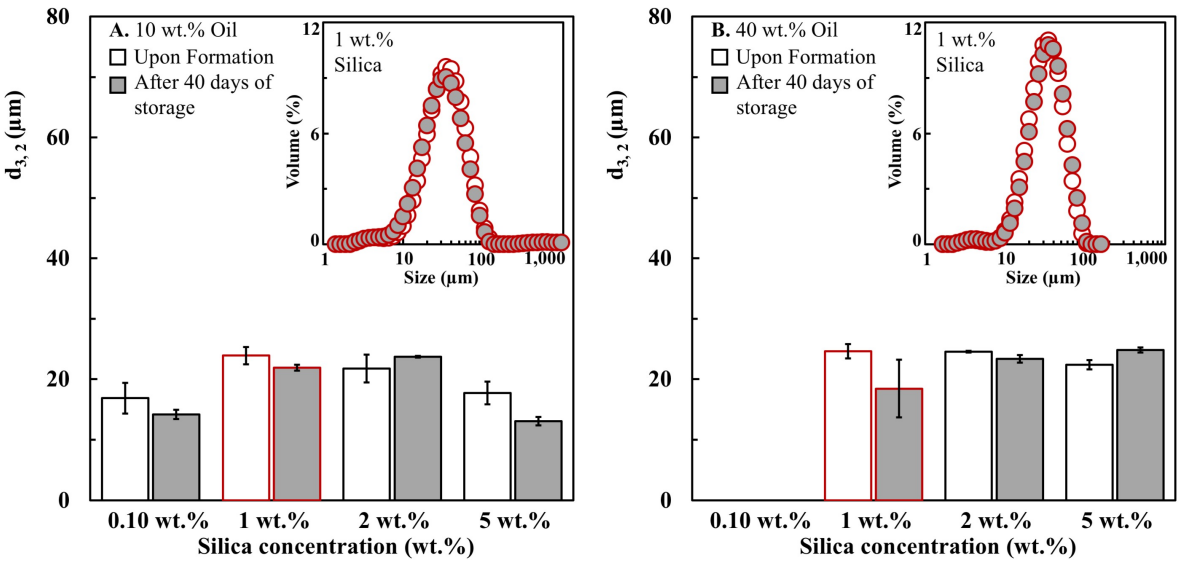

Figure 6. Long-term stability of emulsions manufactured following a single pass within the CIJs device (at a fixed jet flow rate of 352.75 g/min, i.e. corresponding to a $\bar{\varepsilon}_{th}$ (eq.1) equal to ~5×10^3 for 10 wt.% (A) and 40 wt.% (B) oil fraction, respectively) as a function of the silica concentration; concentrations are shown in the graph. The open and solid (grey) bars represent the Sauter diameter ($d_{3,2}$) immediately after the CIJs processing and following the 40 days of storage, respectively. All data points are mean values (n=6) and error bars are reported as a single standard deviation. (Inset chart) Droplet size distributions for the corresponding dispersed phase mass fraction stabilised by 1 wt.% of silica, immediately after the CIJs processing (open symbols) and following the 40 days of storage (solid grey symbols).

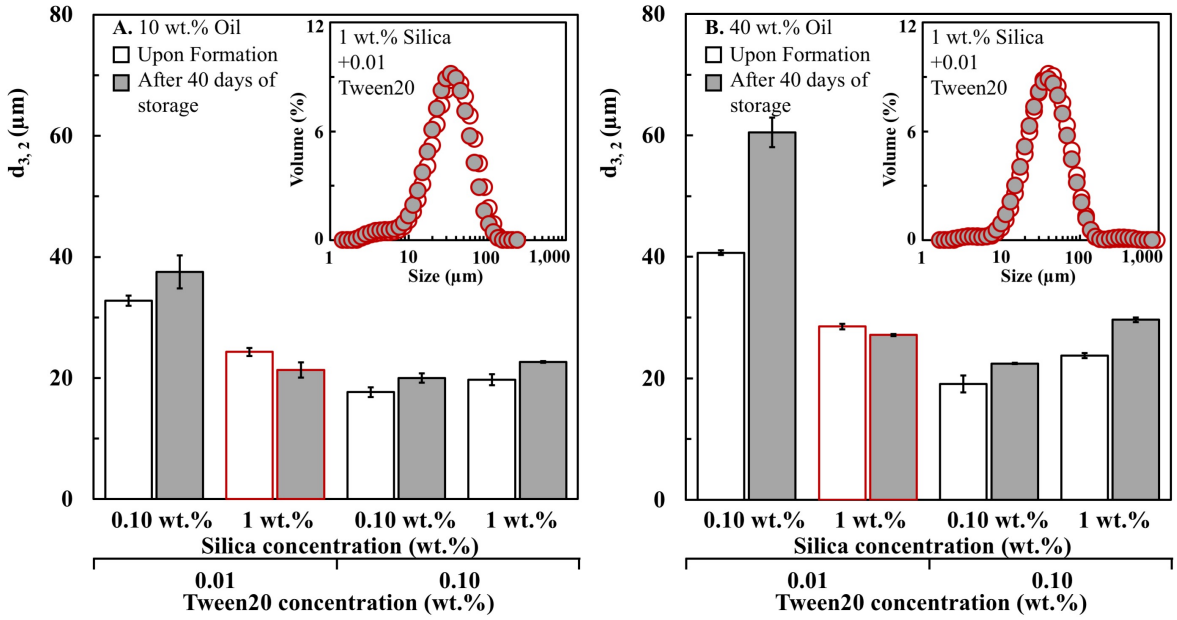

Figure 7. Long-term stability of emulsions manufactured following a single pass within the CIJs device (at a fixed jet flow rate of 352.75 g/min, i.e. corresponding to a $\bar{\varepsilon}_{th}$ (eq. 1) equal to ~5×10^3 for 10 wt.% (A) and 40 wt.% (B) oil fraction, respectively) stabilised by mixed surfactant-particle emulsifier systems; concentrations are shown in the graph. The open and solid (grey) bars represent the Sauter diameter ($d_{3,2}$) immediately after the CIJs processing and following the 40 days of storage, respectively. All data points are mean values (n=6) and error bars are reported as a single standard deviation. (Inset chart) Droplet size distributions for the corresponding dispersed phase mass fraction stabilised 1 wt.% silica combined with 0.01 (A) and 0.10 (B) wt.% of Tween20, immediately after processing (open symbols) and following the 40 days of storage (solid grey symbols).

4. Conclusions

The present study reports for the first time on the preparation of O/W emulsions, stabilised by different concentrations of either Pickering particles alone or mixed emulsifier (surfactant and particles) formulations, using Confined Impinging Jets (CIJs). Systems resulting from the CIJs processing of both dilute (10 wt.%) and semi-concentrated (40 wt.%) pre-emulsions were produced over a range of CIJs hydrodynamic conditions (energy dissipation rates, $\bar{\varepsilon}_{th}$) as well as after multiple passes through the CIJs geometry (recirculation), and their long-term storage stability was assessed.

The average droplet diameter ($d_{3,2}$) of the particle-stabilised systems (for both 10 wt.% and 40 wt.% oil content) was only reduced (from that of their pre-emulsion predecessors) following processing within the previously determined (Tripodi *et al.*, 2019) optimal (in terms of $\bar{\varepsilon}_{th}$) CIJs operation window, reaching the smallest $d_{3,2}$ (~10µm) under fully turbulent conditions, regardless of the particle concentration used. Emulsions stabilised by the mixed (surfactant and particles) emulsifier formulations also followed this trend, with systems at the lowest concentration (0.01 wt.% Tween20 and 0.10 wt.% silica) being the only exception. The latter gave emulsions of either practically unchanged (at a 10 wt.% oil content) or increasing (at a 40 wt.% oil content) $d_{3,2}$ values at CIJs hydrodynamic conditions of higher $\bar{\varepsilon}_{th}$. Multi-passing of these systems through the CIJs geometry (at an intermediate, but still within

optimal operation, fixed $\bar{\varepsilon}_{th}$) demonstrated that the original (1st pass) emulsion droplet diameter is only further reduced following a second passage and that subsequent recirculation attempts had only a minimal effect on emulsion microstructure. In contrast to the requirement for multiple passes (at fixed hydrodynamic conditions) in typical emulsification processes in order to achieve the lowest emulsion droplet size possible, CIJs demonstrated that this can be realised at a much earlier processing stage and therefore at a reduced expenditure in terms of energy input. Finally, emulsion stability was shown to be driven by formulation rather than processing aspects. The concentration of the particle or mixed emulsifier stabilising intervention was mainly responsible for ensuring that emulsion stability was maintained over the studied 40 days storage period, while CIJs hydrodynamic conditions and multi-passing primarily control the final droplet size and droplet size distribution.

In conclusion, this study extends the effectiveness of CIJs as an easy-to-operate tool to promote a turbulent emulsification environment and allow for the manufacture of a large array of emulsions (including Pickering emulsions) under a wide range of processing conditions. The potential of CIJs to produce a wide spectrum of emulsion microstructures together with the process's lower-energy credentials and capacity to deliver high product throughputs, are progressively enhancing its industrial applicability.

ABBREVIATIONS

CIJs, Confined Impinging Jets; HLB, Hydrophilic Lipophilic Balance

SYMBOLS

$d_{3,2}$	Sauter diameter (m)
Q_{jet}	Volumetric jet flow rate (m^3/s)
V_{CIJs}	CIJs chamber volume where jet collision takes place (m^3)
W_{jet}	Mass jet flow rate (Kg/s)
γ	Equilibrium interfacial tension (N/m)
ΔP	Pressure at which jet collision takes place (Pa)
$\bar{\varepsilon}_{th}$	Theoretically calculated energy dissipation rate (W/Kg)
ρ	Density of the pre-emulsion

AUTHOR CONTRIBUTION

The manuscript was written through contributions of all authors. All authors have given approval to the final version of the manuscript.

AUTHOR INFORMATION

*Ernesto Tripodi, School of Chemical Engineering, University of Birmingham, B15 2TT Birmingham, United Kingdom.

ACKNOWLEDGMENTS

This research was funded by the Centre for Innovative Manufacturing (CIM) in Food and the Engineering and Physical Science Research Council (EP/K030957/1).

References

Aveyard, R. , Binks, B. P. & Clint, J. H. 2003. Emulsions stabilised solely by colloidal particles. Adv. Colloids Interface Sci., 100-102, 503-546. https://doi.org/10.1016/S0001-8686(02)00069-6.

Binks, B. P. 2002. Particles as surfactants—similarities and differences. Curr. Opin. Colloid Interface Sci., 7, 21-41. https://doi.org/10.1016/S1359-0294(02)00008-0.

Binks, B. P., Rodrigues, J. A. & Frith, W. J. 2007. Synergistic interaction in emulsions stabilized by a mixture of silica nanoparticles and cationic surfactant. Langmuir, 23, 3626-3636. https://doi.org/10.1021/la0634600.

Chevalier, Y., Bolzinger, M.A. 2013. Emulsions stabilized with solid nanoparticles: Pickering emulsions. Colloid Surface A, 439, 23-34. https://doi.org/10.1016/j.colsurfa.2013.02.054.

Chiou, H., Chan, H.K., Prud'homme, R. K., Raper, J. A. 2008. Evaluation on the use of Confined Liquid Impinging Jets for the synthesis of nanodrug particles. Drug Dev. Ind. Pharm., 34, 59-64. https://doi.org/10.1080/03639040701508011.

Dickinson, E. 2010. Food emulsions and foams: Stabilization by particles. Curr. Opin. Colloid Interface Sci. 15, 40-49. https://doi.org/10.1016/j.cocis.2009.11.001.

Dickinson, E. 2012. Use of nanoparticles and microparticles in the formation and stabilization of food emulsions. Trends Food Sci. Technol. 24, 4-12. https://doi.org/10.1016/j.tifs.2011.09.006.

Donsí, F. 2018. Chapter 11 - Applications of Nanoemulsions in Foods. In: Jafari, S.M., McClements, D. J. (eds.) Nanoemulsions. Academic Press. https://doi.org/10.1016/B978-0-12-811838-2.00011-4.

Floury, J., Desrumaux, A., Lardières, J. 2000. Effect of high-pressure homogenization on droplet size distributions and rheological properties of model oil-in-water emulsions. Innov. Food Sci. Emerg. Technol. 1, 127-134. https://doi.org/10.1016/S1466-8564(00)00012-6.

Huang, Y., Wang, R., Wu, Y., Gao, Z., Dai, C. 2019. Study on stabilizing emulsion by mixing nano-silica and cationic surfactants with different chain length. IOP Conf. Ser. Earth Environ. Sci. 218, 012071. https://doi.org/10.1088/1755-1315/218/1/012071

Hunter, T. N., Pugh, R. J., Franks, G. V. & Jameson, G. J. 2008. The role of particles in stabilising foams and emulsions. Adv. Colloid Interface Sci., 137**,** 57-81.https://doi.org/10.1016/j.cis.2007.07.007

Karbstein, H., Schubert, H. 1995. Developments in the continuous mechanical production of oil-in-water macro-emulsions. Chem. Eng. Process. Issn. 34, 205-211. https://doi.org/10.1016/0255-2701(94)04005-2.

Jafari, S.M., Assadpoor, E., He, Y., Bhandari, B. 2008. Re-coalescence of emulsion droplets during high-energy emulsification. Food Hydrocolloids. 22, 1191-1202. http://doi.org/10.1016/j.foodhyd.2007.09.006.

Kobayashi, I., Mukataka, S., Nakajima, M. 2004. Effect of slot aspect ratio on droplet formation from silicon straight-through microchannels. J. Colloid Interface Sci. 279, 277-280. https://doi.org/10.1016/j.jcis.2004.06.028.

Kralova, I., Sjöblom, J. 2009. Surfactants used in food Industry: A review. J. Disp. Sci. Technol. 30, 1363-1383. http://doi.org/10.1080/01932690902735561.

Leal-Calderon, F. & Schmitt, V. 2008. Solid-stabilized emulsions. Curr. Opin. Colloid Interface Sci, 13**,** 217-227.https://doi.org/10.1016/j.cocis.2007.09.005

Lee, L., Norton, I. T. 2013. Comparing droplet breakup for a high-pressure valve homogeniser and a Microfluidizer for the potential production of food-grade nanoemulsions. J. Food Eng., 114, 158-163. https://doi.org/10.1016/j.jfoodeng.2012.08.009.

McClements, D. J. 2016. Food Emulsions: Principles, Practices and Techniques. Third edition CRC press, Boca Raton.

McClements, D. J., Jafari, S. M. 2018. Improving emulsion formation, stability and performance using mixed emulsifiers: A review. Adv. Colloid Interface Sci., 251, 55-79. https://doi.org/10.1016/j.cis.2017.12.001.

Midmore, B. R. 1998. Synergy between silica and polyoxyethylene surfactants in the formation of O/W emulsions. Coll. Surf. A. 145, 133-143. https://doi.org/10.1016/S0927-7757(98)00577-9.

Nesterenko, A., Drelich, A., Lu, H., Clausse, D., Pezron, I. 2014. Influence of a mixed particle/surfactant emulsifier system on water-in-oil emulsion stability. Coll. Surf. A. 457, 49-57. https://doi.org/10.1016/j.colsurfa.2014.05.044.

Pichot, R., Spyropoulos, F., Norton, I. T. 2009. Mixed-emulsifier stabilised emulsions: Investigation of the effect of monoolein and hydrophilic silica particle mixtures on the stability against coalescence. J. Coll. Interf. Sci. 329, 284-291. https://doi.org/10.1016/j.jcis.2008.09.083.

Qian, C., McClements, D. J. 2011. Formation of nanoemulsions stabilized by model food-grade emulsifiers using high-pressure homogenization: Factors affecting particle size. Food Hydrocolloids, 25, 1000-1008. https://doi.org/10.1016/j.foodhyd.2010.09.017.

Ravera, F., Ferrari, M., Liggieri, L., Loglio, G., Santini, E., Zanobini, A. 2008. Liquid–liquid interfacial properties of mixed nanoparticle–surfactant systems. Coll. Surf. A. 323, 99-108. https://doi.org/10.1016/j.colsurfa.2007.10.017.

Rayner, M. 2015. Scales and Forces in Emulsification. In: Rayner, M. & Dejmek, P. (eds.) Engineering Aspects of Food Emulsification and Homogenisation. CRC press. Boca Raton. http://doi.org/10.1201/b18436-3.

Tcholakova, S., Denkov, N. D., Lips, A. 2008. Comparison of solid particles, globular proteins and surfactants as emulsifiers. Phys. Chem. Chem. Phys. 10, 1608-1627. http://doi.org/10.1039/B715933C.

Tesch, S., Gerhards, C. & Schubert, H. 2002. Stabilization of emulsions by OSA starches. J. Food Eng. 54, 167-174. https://doi.org/10.1016/S0260-8774(01)00206-0.

Siddiqui, S. W., Zhao, Y., Kukukova, A., Kresta, S. M. 2009. Characteristics of a Confined Impinging Jet Reactor: energy dissipation, homogeneous and heterogeneous reaction products, and effect of unequal flow. Ind. Eng. Chem. Res. 48, 7945-7958. http://doi.org/10.1021/ie801562y.

Siddiqui, S. W., Norton, I. T. 2012. Oil-in-water emulsification using Confined Impinging Jets. J. Coll. Interf. Sci. 377, 213-221. https://doi.org/10.1016/j.jcis.2012.03.062.

Siddiqui, S. W., Wan Mohamad, W. A. F., Mohd. Rozi, M. F., Norton, I. T. 2017. Continuous, high-throughput flash-synthesis of submicron food emulsions using a Confined Impinging Jet Mixer: effect of in situ turbulence, sonication, and small surfactants. Ind. Eng. Chem. Res. 56, 12833-12847. http://doi.org/10.1021/acs.iecr.7b02124.

Tripodi, E., Lazidis, A., Norton, I. T., Spyropoulos, F. 2019. On the production of oil-in-water emulsions with varying dispersed phase content using Confined Impinging Jet Mixers. Ind. Eng. Chem. Res. 58, 14859-14872. http://doi.org/10.1021/acs.iecr.9b00634.

Vashisth, C., Whitby, C. P., Fornasiero, D., Ralston, J. 2010. Interfacial displacement of nanoparticles by surfactant molecules in emulsions. J. Coll. Interf. Sci., 349, 537-543. https://doi.org/10.1016/j.jcis.2010.05.089.

Vladisavljević, G. T., Kobayashi, I., Nakajima, M. 2012. Production of uniform droplets using membrane, microchannel and microfluidic emulsification devices. Microfluid. Nanofluidics, 13, 151-178. http://10.1007/s10404-012-0948-0.

Walstra, P. 1993. Principles of emulsion formation. Chem. Eng. Sci. 48, 333-349. https://doi.org/10.1016/0009-2509(93)80021-H.

Zafeiri, I., Horridge, C., Tripodi, E., Spyropoulos, F. 2017. Emulsions co-stabilised by edible Pickering particles and surfactants: the effect of HLB value. Coll. Interf. Sci. Comm., 17, 5-9. https://doi.org/10.1016/j.colcom.2017.02.001.